Analytica Chimica Acta 1161 (2021) 338326

Contents lists available at ScienceDirect

Analytica Chimica Acta

journal homepage: www.elsevier.com/locate/aca

Molecularly imprinted fluoroprobes doped with Ag nanoparticles for highly selective detection of oxytetracycline in real samples

Jixiang Wang [a, b], Lihua Zou [c], Jingjing Xu [c, **], Rong Zhang [d, ***], Hongbo Zhang [a, b, *]

[a] Pharmaceutical Sciences Laboratory, Åbo Akademi University, FI-20520, Turku, Finland
[b] Turku Bioscience Centre, University of Turku and Åbo Akademi University, FI-20520, Turku, Finland
[c] Center for Molecular Recognition and Biosensing, School of Life Sciences, Shanghai University, Shanghai, 200444, PR China
[d] Department of Interventional Radiology, Shanghai Jiao Tong University Affiliated Sixth People's Hospital, CN-200233, Shanghai, PR China

HIGHLIGHTS

- Ag nanoparticles promote electron/energy transfer, leading to high reaction speed.
- Molecularly imprinted fluoroprobes (SiO_2/Ag@FMIPs) are successfully prepared.
- SiO_2/Ag@FMIPs exhibit a LOD low to 5.38 nM within 2.5 min toward OTC in real samples.

GRAPHICAL ABSTRACT

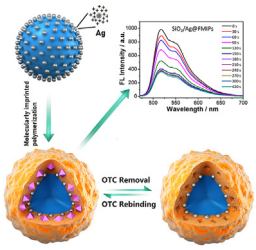

ARTICLE INFO

Article history:
Received 11 December 2020
Received in revised form
12 February 2021
Accepted 13 February 2021
Available online 6 March 2021

Keywords:
Molecularly imprinted polymer
Oxytetracycline
Fluorescence detection
Rapid analysis
Ag nanoparticle

ABSTRACT

A molecularly imprinted polymer (MIP), which is synthesized by a nanomolding process around a template, has emerged as a promising analytical tool for environmental quality monitoring and food safety test. In this work, a fluoroprobe with Ag-doped MIP nanolayer (16 nm thickness) is successfully prepared for the highly selective detection of oxytetracycline (OTC) in real samples (i.e. Yangtze River water, swine urine). In the MIP nanolayer, two functional monomers (i.e. 4-(2-acrylamidoethylcarbamoyl)-3-fluorophenylboronic acid, methacrylic acid) synergistically constitute the specific recognition sites. Meanwhile, the doped Ag enhances the detection sensitivity (with a detection limit of 5.38 nM) and accelerates the detection rate (within 2.5 min) even in real samples. Therefore, the present study paves the way for the preparation of MIP-based fluoroprobes, showing great prospects in environmental quality and food safety tests.

1. Introduction

Oxytetracycline (OTC), a sort of broad-spectrum antibiotics belonging to the tetracycline family, is widely used in the animal breeding industry as a veterinary drug and growth promoter for the prevention and control of animal diseases [1]. According to the statistics worldwide, 2000 tons of OTC are used in animal husbandry and aquaculture every year. As applied on a large scale, OTC in animal-derived foods and drinking water has potentially severe effects on human health, such as allergic reactions, toxic effects, and the resistance toward antibiotics [2]. Thus, there is an increasing concern over the negative effects of inappropriate antibiotic use, which brings a growing demand for on-site diagnosis of

* Corresponding author. Pharmaceutical Sciences Laboratory, Åbo Akademi University, FI-20520, Turku, Finland.
** Corresponding author.
*** Corresponding author.
E-mail addresses: jingjing_xu@shu.edu.cn (J. Xu), rongzhang@163.com (R. Zhang), hongbo.zhang@abo.fi (H. Zhang).

https://doi.org/10.1016/j.aca.2021.338326

antibiotic residues in environmental water and animal-derived foods [3].

In recent years, significant efforts have been made to OTC detection [4]. Particularly, the fluorescence sensors that exhibit considerable advantages over traditional chromatographic methods [5], including little consumption of samples, inexpensive equipment and on-site detection convenience, have drawn a great attention [6]. However, the traditional fluorescence sensors are difficult to apply to real sample detection, due to the limited selectivity of ordinary recognition elements [7,8]. To overcome this drawback, the incorporation of sensitive fluorophore in a highly selective molecularly imprinted polymer (MIP) may effectively eliminate the interference of coexisting substances [9–13]. The MIP is a synthetic receptor made for a target molecule, with recognition sites complementary in size, shape, and chemical functionality toward the target molecule [14]. If the MIP contains a sensitive fluorophore (referred as FMIP) in the recognition sites, it may not only specifically identify the target molecule, but also exhibit fluorescent signal for on-site quantification analysis [15]. Though, the FMIPs have made tremendous progress in accurately detecting analyte in real samples [16], they also remain some inevitable issues to be addressed, especially regarding their long reaction time. For example, the fluorophore in the excited state interacts with the target quencher, resulting in the fluorescence quenching phenomenon [17]. If the target quencher takes a long time to enter the recognition sites, besides the process of quenching is usually slow, the detection rate may last nearly 1 h [18,19]. Therefore, the development of efficient FMIPs for OTC detection is of great importance.

To overcome the aforementioned issues, we developed a thin-walled MIP that possesses accessible recognition sites located at the surface, so as to improve the binding kinetics [20,21]. Meanwhile, Ag nanoparticles that promote electron/energy transfer were incorporated to increase the reaction speed of fluorescence quenching [22–24]. Specifically, we prepared the fluoroprobes by synthesizing Ag-doped ultrathin FMIPs on SiO_2 particles (referred as SiO_2/Ag@FMIPs, Scheme 1) and applied the fluoroprobes for the detection of OTC in real samples: Yangtze River water and swine urine. In this work, a new fluorescent functional monomer 2-(6-(allyloxy)-3-oxo-3H-xanthen-9-yl) benzoate (AOXB) was used as the fluorophore for FMIP synthesis. The novel fluoroprobes employed two functional monomers (i.e. 4-(2-acrylamidoethylcarbamoyl)-3-fluorophenylboronic acid, referred as AFPBA; methacrylic acid, referred as MAA) for specific recognition of OTC, by forming a large number of hydrogen bonds, ionic bonds, etc, in a very small space. Moreover, the positron cloud generated by Ag nanoparticles led to the accelerated detection rate of OTC, with respect to control fluoroprobes (SiO_2@FMIPs). The results showed the excellent selectivity of our SiO_2/Ag@FMIPs as fluorophores for detecting antibiotics in real samples in the nM range within 2.5 min.

2. Materials and methods

2.1. Preparation of fluoroprobes

Preparation of SiO_2 particles. Stöver method is used to prepare SiO_2 particles. Briefly, $NH_3 \cdot H_2O$ (28%, 0.2 mL), ethanol (2.5 mL), and double-distilled water (2.5 mL) were mixed and stirred at room temperature for 30 min. Then, tetraethyl orthosilicate (TEOS, 0.2 mL) was dropped into the solution and stirred at room temperature for 24 h. At the end, the SiO_2 particles were obtained by centrifugation (12000 rpm, 30 min) and drying at 60 °C.

Preparation of SiO_2/Ag nanoparticles. Typically, the $AgNO_3$ (0.1 mmol/L) and polyvinyl pyrrolidone (PVP, MW: 10 kDa, 0.2 mmol/L) solutions were pre-configured for use. The SiO_2 (all products obtained in the previous step) were dispersed in a solvent composed of double-distilled water (10 mL) and ethanol (40 mL) by ultrasound for 30 min. Then, the pre-configured $AgNO_3$ solution (2.5 mL) was slowly added into the SiO_2 suspension, followed by stirring for 3 min. Subsequently, the pre-configured PVP solution (2.5 mL) was added to the suspension in dark, with stirring at room temperature for 4 h. Then, ethanolamine (250 μL) was added and stirred in dark at 71 °C for 12 h. Finally, the SiO_2/Ag nanoparticles were collected by centrifugation and washing with ethanol and water for several times, followed by vacuum drying at 35 °C for 5 h.

Preparation of SiO_2/Ag@FMIPs, SiO_2/Ag@FNIPs, SiO_2@FMIPs. To generate polymer layer on the surface of silica, a modification with double bonds is essential. So, the obtained SiO_2/Ag nanoparticles were dispersed in methylbenzene (anhydrous, 50 mL). Then, 3-(methacryloxyl) propyl trimethoxysilane (KH-570, 1.0 mL) was dripped into the SiO_2/Ag nanoparticles suspension and stirred at 90 °C for 12 h. Finally, the SiO_2/Ag−KH570 were collected by centrifugation and dried at 60 °C for 10 h. In this study, we used precipitation polymerization method to prepare SiO_2/Ag@FMIPs. First, the obtained SiO_2/Ag−KH570 were dispersed in acetonitrile (anhydrous, 40 mL) for further used. The pre-polymerization mixture was prepared by using AOXB (30 mg), OTC (0.1 mmol, 49.65 mg), 4-(2-acrylamidoethylcarbamoyl)-3-fluorophenylboronic acid (AFBPA, 0.2 mmol, 56 mg), methacrylic acid (MAA, 0.2 mmol, 17.218 mg), and ethylene glycol dimethacrylate (EGDMA, 0.4 mmol, 79.28 mg) solubilized in acetonitrile (20 mL) and maintained stationary for 12 h in the dark. Afterward, the pre-polymerization mixture was slowly added into the SiO_2/Ag−KH570 suspension and stirred for 15 min. After purging with nitrogen for 30 min, an initiator 2, 2′-azobis (isobutyronitrile) (AIBN, 10 mg) was added for polymerization at 60 °C for 24 h. Finally, the SiO_2/Ag@FMIPs were obtained after template elution by dialyzing in acetic acid/methanol (100 mL, 1:9, v/v) for 5 days, followed by centrifugation and vacuum-drying at 40 °C for 5 h. The non-imprinted polymers (NIPs) were synthesized on the SiO_2/Ag−KH570 (referred as SiO_2/Ag@FNIPs) in the same way without the presence of OTC. The SiO_2@FMIPs without doped Ag were prepared by following the same protocol as well, by using SiO_2 instead of SiO_2/Ag−KH570.

2.2. Characterization of fluoroprobes

Characterization of SiO_2/Ag@FMIPs, SiO_2/Ag@FNIPs, SiO_2@FMIPs. The synthesized SiO_2, SiO_2/Ag@FMIPs and SiO_2/Ag@FNIPs were analyzed by the X-ray photoelectron spectroscopy the thermogravimetric analysis (TGA) experiment for verifying polymer coating. Then, the morphologies of SiO_2, SiO_2/Ag, SiO_2/Ag@FMIPs, and SiO_2@FMIPs were investigated by scanning electron microscopy (SEM), transmission electron microscopy (TEM), and the corresponding sizes were confirmed by dynamic light scattering (DLS) test. Meanwhile, the scanning transmission electron microscope (STEM) was employed. For fluorescent imaging analysis, a confocal laser scanning microscope (CLSM, TCS SP5 II laser confocal microscopy (Leica, Germany) with a 488 nm solid state laser light source) was used, later evaluated by the Grayscale analysis software.

2.3. Detection performance of fluoroprobes

Specificity test. For fluorescence intensity measurements, Cary Eclipse fluorescence spectrophotometer (Varian, USA) was used. The fluorescence intensity was read at room temperature with excitation wavelength set at 488 nm. After incubation with OTC, the fluorescence quenching ratio (F_0/F) of fluoroprobes was recorded at 525 nm. Specifically, SiO_2/Ag@FMIPs and SiO_2/Ag@FNIPs (7.0 mg/

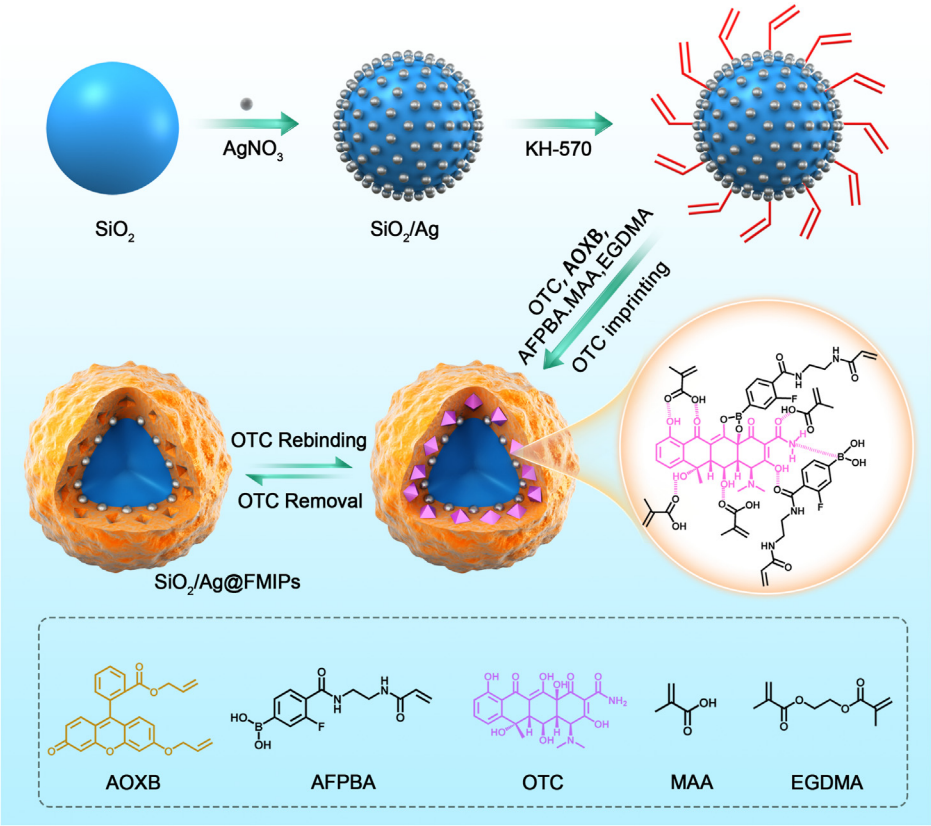

Scheme 1. Schematic representation of SiO_2/Ag@FMIPs synthesis with specific recognition sites for OTC. KH-570 represents 3-(methacryloxyl) propyl trimethoxysilane.

mL) were incubated with OTC at concentrations of 0, 10, 20, 40, 80, 150, 300, 600, 1200, 2400, 3500 nM at room temperature for 10 min, respectively. Then, fluorescence intensity of each sample was recorded on the Cary Eclipse fluorescence spectrophotometer for further analysis. In addition, the dynamic binding kinetic study was performed on a Quanta Master™ 40 Spectrofluorometer (Photon Technology International, U.S.A). SiO_2/Ag@FMIPs and SiO_2/Ag@FNIPs (7.0 mg/mL) were incubated with OTC (300 nM), the fluorescent change was tracked on the Quanta Master™ 40 Spectrofluorometer until quenching equilibration.

Selectivity test. Two structural analogs (antibiotics), which are levofloxacin (LEV) and amoxicillin (AMO), were used to compare with OTC detection. SiO_2/Ag@FMIPs and SiO_2/Ag@FNIPs (7.0 mg/mL) were incubated with OTC, or LEV, or AMO, or OTC + LEV + AMO (taking three antibiotics as an entirety here) at concentrations of 0, 10, 20, 40, 80, 150, 300 nM, respectively. Then, fluorescence intensity of each sample was recorded on the Cary Eclipse fluorescence spectrophotometer for comparison.

Real samples detection. The Yangtze River water and swine urine were collected. Then, a standard recovery method was adopted, using a calibration plot. For spiked samples preparation, a standard OTC at different concentrations (0–300 nM) was prepared either in Yangtze River water or in 100 × diluted swine urine, for the determination of recovery. Samples were centrifuged to remove insoluble impurities or proteins before Cary Eclipse fluorescence spectrophotometer tests.

3. Results and discussion

3.1. Characterization of fluoroprobes

The morphologies of SiO_2, SiO_2/Ag, and SiO_2/Ag@FMIPs were investigated by SEM, TEM, and the corresponding sizes were confirmed by DLS test (Fig. 1a, Figs. S3 and S4). As an inorganic core, SiO_2 has a smooth and uniform surface, a regular spherical morphology, and optimal monodispersity at an average diameter of ~325 nm. After polyvinyl pyrrolidone-induced Ag^+ reduction, the in-situ Ag nanoparticles were uniformly distributed on the surface of SiO_2. SiO_2/Ag@FMIPs displayed a clear core-shell structure with an average size of ~365 nm. The FMIP nanplayer was coated on the surface of SiO_2/Ag, and the majority of the Ag nanoparticles were wrapped inside the imprinted layer (thickness of 16 nm). Meanwhile, the STEM and elemental distribution mapping images of SiO_2/Ag@FMIPs were performed (Fig. 1b), which further validated the incorporation of Ag nanoparticles.

To see more in detail, the SiO_2, SiO_2/Ag, and SiO_2/Ag@FMIPs were tested by the XPS for composition analysis (Fig. S5). In the blue curve, the C—OH, O—C—O, O—C, and O═C in O1s peaks validated the presence of AOXB in SiO_2/Ag@FMIPs. The binding peaks of N1s and F1s showed evidence of AFPBA and MAA. Thus, the SiO_2/Ag@FMIPs were successfully prepared, which exhibited an excellent thermal stability even at 350 °C.

For fluorescent property analysis, the images of SiO_2/Ag@FMIPs before and after OTC detection were captured by the CLSM, then evaluated by the Grayscale analysis software (Fig. 2a and b, Table 1). Unlike those without OTC, the fluorescence intensity of SiO_2/Ag@FMIPs bound to OTC was markedly weak, indicating the fluorescence quenching mechanism for OTC detection. Usually, the

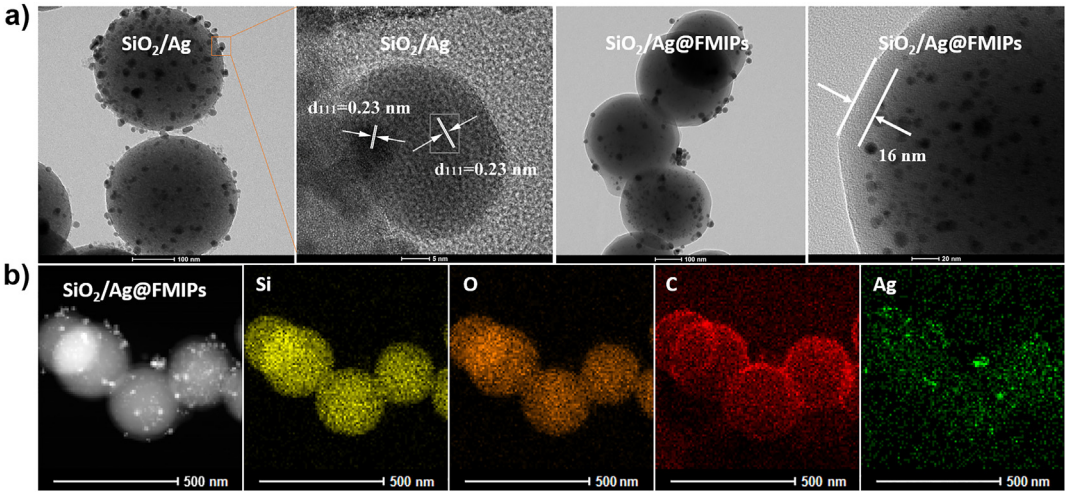

Fig. 1. (a) TEM images. (b) STEM image of SiO_2/Ag@FMIPs and elemental distribution mapping of Si, O, C and Ag elements.

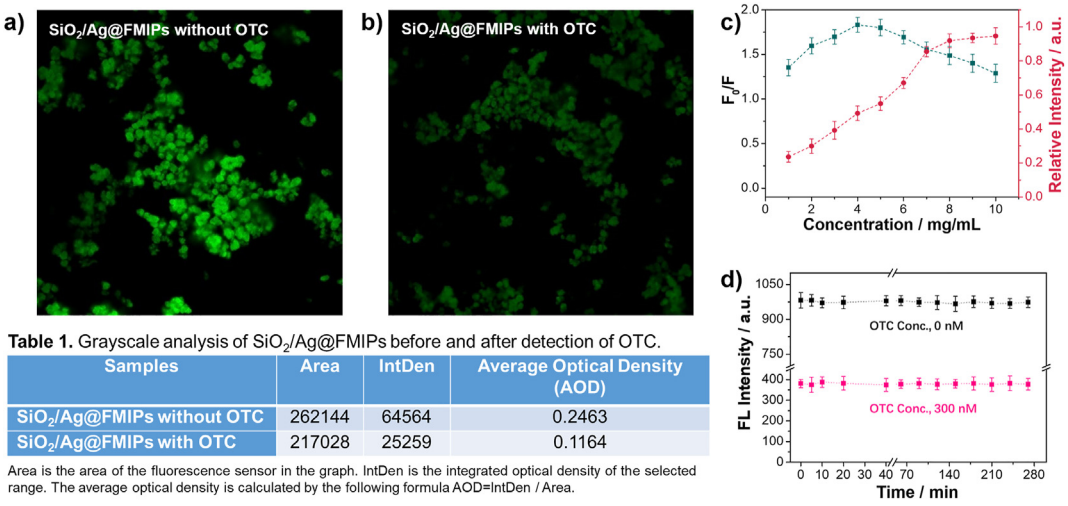

Table 1. Grayscale analysis of SiO_2/Ag@FMIPs before and after detection of OTC.

Samples	Area	IntDen	Average Optical Density (AOD)
SiO_2/Ag@FMIPs without OTC	262144	64564	0.2463
SiO_2/Ag@FMIPs with OTC	217028	25259	0.1164

Area is the area of the fluorescence sensor in the graph. IntDen is the integrated optical density of the selected range. The average optical density is calculated by the following formula AOD=IntDen / Area.

Fig. 2. CLSM and grayscale analysis images of a) SiO_2/Ag@FMIPs without OTC; b) SiO_2/Ag@FMIPs with 3.5 μM OTC (Grayscale analysis results summarized in Table 1). c) Effects of the SiO_2/Ag@FMIPs concentration on fluorescence intensity. Green curve: the fluorescence quenching ratio of the detection system (containing SiO_2/Ag@FMIPs & OTC) *vs.* SiO_2/Ag@FMIPs concentration. Red curve: the fluorescence intensity *vs.* SiO_2/Ag@FMIPs concentration. d) Stability of SiO_2/Ag@FMIPs in PBS without and with OTC bound. Error bars represent the standard deviation of uncertainty (n = 3). (For interpretation of the references to colour in this figure legend, the reader is referred to the Web version of this article.)

Table 1
Grayscale analysis of SiO_2/Ag@FMIPs before and after detection of OTC.

Samples	Area	IntDen	Average Optical Density (AOD)
SiO_2/Ag@FMIPs without OTC	262144	64564	0.2463
SiO_2/Ag@FMIPs with OTC	217028	25259	0.1164

Area is the area of the fluorescence sensor in the graph. IntDen is the integrated optical density of the selected range. The average optical density is calculated by the following formula AOD = IntDen/Area.

level of fluoroprobes has a great influence on the detection sensitivity. If the concentration of fluoroprobes is extremely high, the distance between the fluoroprobes decreases, which results in self-quenching and low sensitivity. On the contrary, the linear range for target detection will be very narrow, leading to poor accuracy. To investigate the appropriate concentration of fluoroprobes, the SiO_2/Ag@FMIPs were prepared at the concentration range of 1.0–10 mg/mL for 80 nM OTC detection in Milli-Q water. As shown in Fig. 2c, although the relative fluorescence intensity of SiO_2/Ag@FMIPs kept increasing upon binding toward OTC, the fluorescence quenching ratio (F0/F, where F0 is the fluorescence intensity of fluoroprobes in the absence of OTC, F is that in the presence of OTC) reached maximum at 4.0 mg/mL. In order to meet the detection requirements, both the fluorescence intensity and the quenching ratio should be considered, the two curves were plotted and found to intercross at the concentration of 7.0 mg/mL, which was then applied in following tests. Then, the fluorescence stability of our fluoroprobes was explored during 270 min. According to Fig. 2d, the SiO_2/Ag@FMIPs without OTC or with OTC maintained the fluorescence intensity over a prolonged period, demonstrating the

excellent stability.

3.2. Specificity test

Using the synthesized fluoroprobes (working concentration: 7.0 mg/mL), the detecting performance was investigated by tracking the fluorescence response upon binding toward OTC. As shown in Fig. 3a and d, the fluorescence intensity of SiO_2/Ag@FMIPs gave a sharper fall in the presence of OTC at concentrations from 10 to 3500 nM, with respect to SiO_2/Ag@FNIPs. This difference between MIP and NIP indicates the creation of specific imprinted sites. Moreover, the linear correlation of the fluorescence quenching ratio versus OTC concentration was displayed in Fig. 3b and e. The results demonstrate that SiO_2/Ag@FMIPs exhibited an excellent linear correlation within the 0–300 nM for OTC detection. On the other hand, the linearity of SiO_2/Ag@FNIPs detection results was very poor, probably because of the disorderly arranged functional monomers. Specifically, AOXB (Fig. S1) was used as the fluorophore incorporated in FMIP, which played an important role in fluorescence quenching upon binding toward OTC. AFPBA (Fig. S2) was applied as the functional monomer to imprint OTC, which formed intermolecular B–N coordination with amino groups in OTC and exhibited boron affinity toward OTC under neutral conditions. Furthermore, MAA can form ionic and hydrogen bonds with carbonyl and hydroxyl groups in OTC structure. So, the hydrogen bond, ionic bond, boron affinity bond and intermolecular B–N coordination all together made a specific recognition performance. According to the equation: $D = 3\sigma/k$ (where σ is the relative standard deviation of the blank sample, k is the slope of the calibration line), the limit of detection (LOD) for SiO_2/Ag@FMIPs was calculated to be 5.38 nM, 5 times lower than that of SiO_2/Ag@FNIPs.

Furthermore, the dynamic binding property of fluoroprobes toward 300 nM OTC was studied as well. Comparing Fig. 3c and f, it is interesting to note that SiO_2/Ag@FMIPs showed a fluorescence quenching rate much higher than that of SiO_2/FMIPs, by using only 150 s to reach an equivalent fluorescence quenching, with respect to 450 s in the other case. This phenomenon was probably attributed to the fact that the SiO_2/Ag@FMIPs were doped with Ag nanoparticles which may distribute near the recognition sites. Since the Ag nanoparticles promote the energy/electron transfer due to the surrounding positron cloud, leading to the accelerated fluorescence quenching (Fig. S6) [25]. Compared to other OTC detection methods [26], our SiO_2/Ag@FMIPs exhibit significant advances, i.e. a wide detection range with LOD in nM level, detection time within 2.5 min.

3.3. Selectivity test

In order to study the anti-interference ability of the SiO_2/Ag@FMIPs, the potential interferences that are similar in structure with OTC: levofloxacin (LEV) and amoxicillin (AMO) were used to compare with OTC. As shown in Fig. 4, that the fluorescence quenching efficiency of SiO_2/Ag@FMIPs to other structural analogs was much lower than that to OTC. Particularly, when SiO_2/Ag@FMIPs were incubated with OTC, LEV and AMO mixture, they gave almost the same quenching efficiency with respect to OTC alone, demonstrating their great potentials in anti-interference detecting. On the other hand, SiO_2/Ag@FNIPs exhibited finite differences toward three antibiotics, and significant high quenching efficiency toward their mixture. Therefore, based on the excellent detection performance, our SiO_2/Ag@FMIPs are promising to distinguish OTC in real samples.

3.4. Real samples detection

Since SiO_2/Ag@FMIPs exhibit high sensitivity and excellent selectivity for OTC, they were then used for the determination of OTC in real samples. Herein, we collected Yangtze River water/swine urine as OTC-containing practical samples. Since the OTC is often used in animal husbandry, especially swine husbandry. Thus, swine eats abundant OTC-containing feed, which will inevitably increase the OTC level in the body. So, instead of monitoring the OTC content in swine agricultural products, we used swine urine from local farms for more convenient analysis. Using the standard

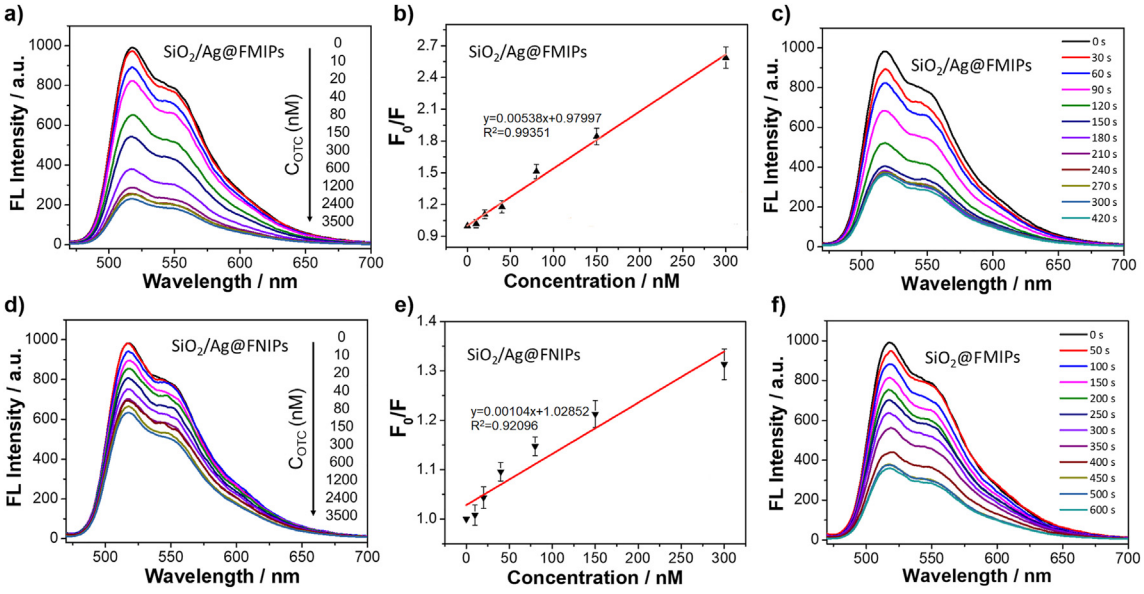

Fig. 3. (a, d) Analyte-dependent fluorescence emission spectra of SiO_2/Ag@FMIPs and SiO_2/Ag@FNIPs with respect to OTC ranging from 0 to 3.5 μM. (b, e) Lear fitting plot of fluorescence quenching ratio of SiO_2/Ag@FMIPs and SiO_2/Ag@FNIPs toward OTC ranging from 0 to 300 nM. Error bars represent the standard deviation of uncertainty (n = 3). (c, f) Quenching time analysis for dynamic binding kinetic study of SiO_2/Ag@FMIPs and SiO_2@FMIPs toward 300 nM OTC. Experimental conditions: concentrations of SiO_2/Ag@FMIPs, SiO_2/Ag@FNIPs, SiO_2@FMIPs are 7.0 mg/mL in PBS, pH 7.4. Excitation wavelength: 488 nm.

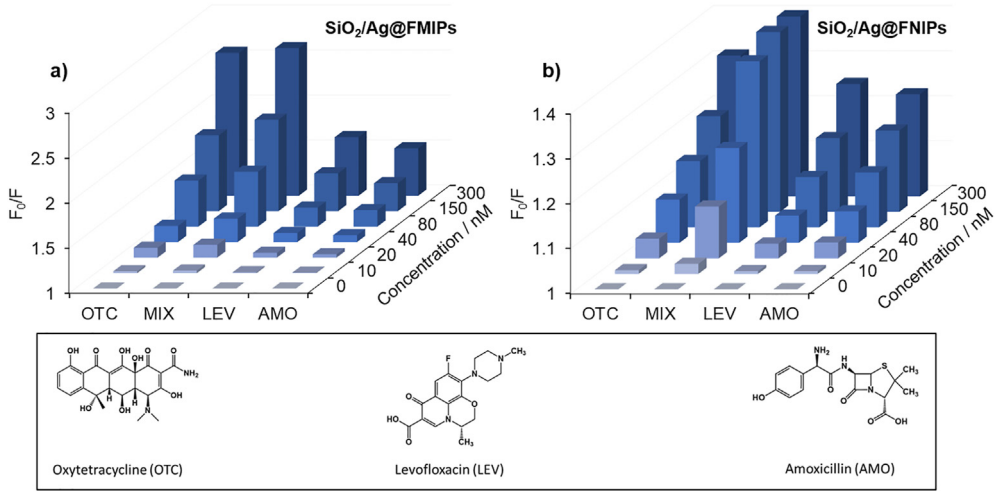

Fig. 4. Fluorescence quenching performance of SiO_2/Ag@FMIPs (a) and SiO_2/Ag@FNIPs (b) toward three antibiotics at the concentration range of 0–300 nM, as well as a mixture of three antibiotics at the same concentrations. The chemical structure formula of three antibiotics are given below (n = 3).

Table 2
Ratiometric determination of OTC in Yangtze River water using SiO_2/Ag@FMIPs.

Sample	Spiked (nM)	Detected (nM)	Recovery (%)[a]	RSD (%, n = 3)
Yangtze River water	0	0	–	
	20	18.4	92.0	12.4
	40	40.7	101.8	10.1
	80	82.2	102.7	5.8
	150	152.6	101.7	3.5
	300	309.5	103.2	2.4

Table 3
Ratiometric determination of OTC in swine urine samples using SiO_2/Ag@FMIPs.

Sample	Spiked (nM)	Detected (nM)	Recovery (%)[a]	RSD (%, n = 3)
Swine urine	0	0.2	–	–
	20	24.4	122.0	17.1
	40	46.3	115.8	12.3
	80	87.4	109.2	10.4
	150	158.3	105.5	6.8
	300	316.1	105.4	5.4

[a] In order to reflect the accuracy and preciseness of the experiment, the process was repeated three times, and the average values are presented.

recovery method, OTC at concentrations ranging from 0 to 300 nM were spiked in real samples for the determination of recovery. According to the results of OTC detection in real samples (Tables 2 and 3), our SiO_2/Ag@FMIPs have great potential for similar antibiotics detection in environmental and biological samples.

4. Conclusion

In summary, an Ag-doped OTC-imprinted fluoroprobe was prepared and used for tracing OTC in real samples. The biggest gain in this work is the discovery of the effect of Ag nanoparticles on accelerating the fluorescence quenching reaction. Our SiO_2/Ag@FMIPs are convenient for the highly selective determination of OTC in the nM range within 2.5 min, showing a great potential of this kind of fluoroprobes in the detection of similar antibiotics in environmental and biological samples.

CRediT authorship contribution statement

Jixiang Wang: Conceptualization, Writing – original draft, Investigation, Validation, Methodology. **Lihua Zou:** Conceptualization, Writing – original draft, Investigation, Validation, Methodology. **Jingjing Xu:** Conceptualization, Investigation, Writing – review & editing, Supervision, Funding acquisition. **Rong Zhang:** Conceptualization, Supervision. **Hongbo Zhang:** Conceptualization, Investigation, Writing – review & editing, Supervision, Funding acquisition.

Declaration of competing interest

The authors declare that they have no known competing financial interests or personal relationships that could have appeared to influence the work reported in this paper.

Acknowledgements

This work was financially supported by the Sigrid Jusélius Foundation (28001830k1), the Academy of Finland (328933) grants, the National Natural Science Foundation of China (22001162), as well as the Shanghai Sailing Program (No. 20YF1414200). J. Xu thanks the support of the International Research Project METISLAB.

Appendix A. Supplementary data

Supplementary data to this article can be found online at https://doi.org/10.1016/j.aca.2021.338326.

References

[1] J.F. Leal, E.B.H. Santos, V.I. Esteves, Oxytetracycline in intensive aquaculture: water quality during and after its administration, environmental fate, toxicity and bacterial resistance, Rev. Aquacult. 11 (2019) 1176–1194.
[2] C. Manyi-Loh, S. Mamphweli, E. Meyer, A. Okoh, Antibiotic use in agriculture and its consequential resistance in environmental sources: potential public health implications, Molecules 23 (2018) 795.
[3] E.K. Silbergeld, J. Graham, L.B. Price, Industrial food animal production, antimicrobial resistance, and human health, Annu. Rev. Publ. Health 29 (2008) 151–169.
[4] (a) B. He, L. Wang, X. Dong, X. Yan, M. Li, S. Yan, D. Yan, Aptamer-based thin film gold electrode modified with gold nanoparticles and carboxylated multi-walled carbon nanotubes for detecting oxytetracycline in chicken samples, Food Chem. 300 (2019);
(b) N. Zhou, Y. Ma, B. Hu, L. He, S. Wang, Z. Zhang, S. Lu, Construction of Ce-MOF@COF hybrid nanostructure: label-free aptasensor for the ultrasensitive detection of oxytetracycline residues in aqueous solution environments, Biosens. Bioelectron. 127 (2019) 92–100;

(c) S. Xu, X. Li, Y. Mao, T. Gao, X. Feng, X. Luo, Novel dual ligand co-functionalized fluorescent gold nanoclusters as a versatile probe for sensitive analysis of Hg^{2+} and oxytetracycline, Anal. Bioanal. Chem. 408 (2016) 2955–2962;
(d) J. Lv, X. Chen, S. Chen, H. Li, H. Deng, A visible light induced ultrasensitive photoelectrochemical sensor based on $Cu_3Mo_2O_9/BaTiO_3$ p-n heterojunction for detecting oxytetracycline, J. Electroanal. Chem. 842 (2019) 161–167;
(e) N. Yildirim-Tirgil, J. Lee, H. Cho, H. Lee, S. Somu, A. Busnaina, A.Z. Gu, A SWCNT based aptasensor system for antibiotic oxytetracycline detection in water samples, Analytical Methods 11 (2019) 2692–2699;
(f) M. Esmaelpourfarkhani, K. Abnous, S.M. Taghdisi, M. Chamsaz, A fluorometric assay for oxytetracycline based on the use of its europium(III) complex and aptamer-modified silver nanoparticles, Microchimica Acta 186 (2019).

[5] S. Li, X. Hu, Q. Chen, X. Zhang, H. Chai, Y. Huang, Introducing bifunctional metal-organic frameworks to the construction of a novel ratiometric fluorescence sensor for screening acid phosphatase activity, Biosens. Bioelectron. 137 (2019) 133–139;
(b) K. Vucicevic-Prcetic, R. Cservenak, N. Radulovic, Determination of neomycin and oxytetracycline in the presence of their impurities in veterinary dosage forms by high-performance liquid chromatography/tandem mass spectrometry, J. AOAC Int. 94 (2011) 750–757;
(c) L. Guo, Y. Chen, L. Zhang, W. Yang, P. He, Development and validation of a liquid chromatographic/tandem mass spectrometric method for determination of chlortetracycline, oxytetracycline, tetracycline, and doxycycline in animal feeds, J. AOAC Int. 95 (2012) 1010–1015;
(d) M.A. Bimazubute, E. Rozet, I. Dizier, J.C. Van Heugen, E. Arancio, P. Gustin, J. Crommen, P. Chiap, Pre-study and in-study validation of an ultra-high pressure LC method coupled to tandem mass spectrometry for off-line determination of oxytetracycline in nasal secretions of healthy pigs, Journal of Chromatography B-Analytical Technologies in the Biomedical and Life Sciences 877 (2009) 2349–2357.

[6] A.C. Sedgwick, L. Wu, H.-H. Han, S.D. Bull, X.-P. He, T.D. James, J.L. Sessler, B.Z. Tang, H. Tian, J. Yoon, Excited-state intramolecular proton-transfer (ESIPT) based fluorescence sensors and imaging agents, Chem. Soc. Rev. 47 (2018) 8842–8880.

[7] X. Wu, Y. Song, X. Yan, C. Zhu, Y. Ma, D. Du, Y. Lin, Carbon quantum dots as fluorescence resonance energy transfer sensors for organophosphate pesticides determination, Biosens. Bioelectron. 94 (2017) 292–297.

[8] J. Pan, W. Chen, Y. Ma, G. Pan, Molecularly imprinted polymers as receptor mimics for selective cell recognition, Chem. Soc. Rev. 47 (2018) 5574–5587.

[9] Q. Yang, J. Li, X. Wang, H. Peng, H. Xiong, L. Chen, Strategies of molecular imprinting-based fluorescence sensors for chemical and biological analysis, Biosens. Bioelectron. 112 (2018) 54–71.

[10] J. Feng, Y. Tao, X. Shen, H. Jin, T. Zhou, Y. Zhou, L. Hu, D. Luo, S. Mei, Y.I. Lee, Highly sensitive and selective fluorescent sensor for tetrabromobisphenol-A in electronic waste samples using molecularly imprinted polymer coated quantum dots, Microchem. J. 144 (2019) 93–101.

[11] L. Liu, X. Tian, Y. Ma, Y. Duan, X. Zhao, G. Pan, A versatile dynamic mussel-inspired biointerface: from specific cell behavior modulation to selective cell isolation, Angew. Chem. Int. Ed. 57 (2018) 7878–7882.

[12] G. Pan, S. Shinde, S.Y. Yeung, M. Jakstaite, Q. Li, A.G. Wingren, B. Sellergren, An epitope-imprinted biointerface with dynamic bioactivity for modulating cell-biomaterial interactions, Angew. Chem. Int. Ed. 56 (2017) 15959–15963.

[13] Z. Tavakoli, M. Soleimani, M.M.A. Nikje, Characterization and performance evaluation of functional monomer effect on molecular imprinted polyurethane foam, J. Chromatogr. A 1602 (2019) 30–40.

[14] J. Xu, H. Miao, J. Wang, G. Pan, Molecularly imprinted synthetic antibodies: from chemical design to biomedical applications, Small 16 (2020) 1906644.

[15] J. Xu, E. Prost, K. Haupt, B.T.S. Bui, Direct and sensitive determination of trypsin in human urine using a water-soluble signaling fluorescent molecularly imprinted polymer nanoprobe, Sensor. Actuator. B Chem. 258 (2018) 10–17.

[16] J. Wang, J. Dai, Y. Xu, X. Dai, Y. Zhang, W. Shi, B. Sellergren, G. Pan, Molecularly imprinted fluorescent test strip for direct, rapid, and visual dopamine detection in tiny amount of biofluid, Small 15 (2019).

[17] S. Niu, Y. Fang, K. Zhang, J. Sun, J. Wan, Determination of dopamine using the fluorescence quenching of 2, 3-diaminophenazine, Instrum. Sci. Technol. 45 (2017) 101–110.

[18] D.-Y. Li, X.-W. He, Y. Chen, W.-Y. Li, Y.-K. Zhang, Novel hybrid structure silica/CdTe/molecularly imprinted polymer: synthesis, specific recognition, and quantitative fluorescence detection of bovine hemoglobin, ACS Appl. Mater. Interfaces 5 (2013) 12609–12616.

[19] D. Gao, Z. Zhang, M. Wu, C. Xie, G. Guan, D. Wang, A surface functional monomer-directing strategy for highly dense imprinting of TNT at surface of silica nanoparticles, J. Am. Chem. Soc. 129 (2007) 7859–7866.

[20] C. Gonzato, M. Courty, P. Pasetto, K. Haupt, Magnetic molecularly imprinted polymer nanocomposites via surface-initiated RAFT polymerization, Adv. Funct. Mater. 21 (2011) 3947–3953.

[21] J. Wang, R. Cheng, Y. Wang, L. Sun, L. Chen, X. Dai, J. Pan, G. Pan, Y. Yan, Surface-imprinted fluorescence microspheres as ultrasensitive sensor for rapid and effective detection of tetracycline in real biological samples, Sensor. Actuator. B Chem. 263 (2018) 533–542.

[22] J. Wang, H. Qiu, H. Shen, J. Pan, X. Dai, Y. Yan, G. Pan, B. Sellergren, Molecularly imprinted fluorescent hollow nanoparticles as sensors for rapid and efficient detection lambda-cyhalothrin in environmental water, Biosens. Bioelectron. 85 (2016) 387–394.

[23] B. Sarkar, K. Ishii, T. Tahara, Microsecond conformational dynamics of biopolymers revealed by dynamic-quenching two-dimensional fluorescence lifetime correlation spectroscopy with single dye labeling, J. Phys. Chem. Lett. 10 (2019) 5536–5541.

[24] W. Stöber, A. Fink, E. Bohn, Controlled growth of monodisperse silica spheres in the micron size range, J. Colloid Interface Sci. 26 (1968) 62–69.

[25] X. Ran, Q. Zhang, Y. Zhang, J. Chen, Z. Wei, Y. He, L. Guo, Probing the electron transfer between iLOV protein and Ag nanoparticles, Molecules 25 (2020) 2544.

[26] (a) H.I.A.S. Gomes, M.G.F. Sales, Development of paper-based color test-strip for drug detection in aquatic environment: application to oxytetracycline, Biosens. Bioelectron. 65 (2015) 54–61;
(b) Y.S. Kim, J.H. Kim, I.A. Kim, S.J. Lee, J. Jurng, M.B. Gu, A novel colorimetric aptasensor using gold nanoparticle for a highly sensitive and specific detection of oxytetracycline, Biosens. Bioelectron. 26 (2010) 1644–1649;
(c) C. Lu, Z. Tang, C. Liu, L. Kang, F. Sun, Magnetic-nanobead-based competitive enzyme-linked aptamer assay for the analysis of oxytetracycline in food, Anal. Bioanal. Chem. 407 (2015), 5859-5859;
(d) J. Sun, T. Gan, W. Meng, Z. Shi, Z. Zhang, Y. Liu, Determination of oxytetracycline in food using a disposable montmorillonite and acetylene black modified microelectrode, Anal. Lett. 48 (2015) 100–115;
(e) H. Zhao, S. Gao, M. Liu, Y. Chang, X. Fan, X. Quan, Fluorescent assay for oxytetracycline based on a long-chain aptamer assembled onto reduced graphene oxide, Microchimica Acta 180 (2013) 829–835.